1-1-1975

Line Detection in Satellite Imagery

G. J. VanderBrug

Reprinted from

Symposium on

Machine Processing of

Remotely Sensed Data

June 3 - 5, 1975

The Laboratory for Applications of
Remote Sensing

Purdue University
West Lafayette
Indiana

IEEE Catalog No.
75CH1009-0 -C

LINE DETECTION IN SATELLITE IMAGERY

G. J. VanderBrug

Computer Science Center
University of Maryland
College Park, Maryland 20742

I. ABSTRACT

Three algorithms for line detection, the linear detector, the nonlinear detector, and the semilinear detector are examined. Experiments are conducted on detecting linear features in terrain on LANDSAT-1 images, and on detecting suburban roads on Skylab images.

II. INTRODUCTION

A class of important features in satellite imagery are the linear features. There are many kinds of linear features; for example, roads, rivers, bridges, vegetation alignments, as well as geologically significant features such as faults and joints. Thus algorithms for locating linear features are of general interest. Bajcsy and Tavakoli [1973, 1974] detect linear features in LANDSAT-1 data which represent major roads, rivers, and bridges.

One class of algorithms for locating linear features in digital pictures involves the use of local operators (detectors). These local line detectors make a decision about the presence of a line at a point by examining only picture points in an immediate neighborhood of the point, and thus (in theory) can be performed in parallel. A second class of algorithms for locating linear features uses more global information. They usually involve some form of line tracking or following, and hence are more sequential in nature.

In this paper we are concerned with local line detectors. Three line detection algorithms are studied, the linear, the nonlinear, and the semilinear algorithms. (For the definitions of these algorithms, see Section II.) The performance of the algorithms is evaluated through the use of a set of experiments using computer generated pictures, Skylab pictures, and LANDSAT-1 pictures. For a comparative study in edge detection in LANDSAT-1 pictures that uses line detectors to enhance the output of edge detectors see [Eberlein et al., 1974].

One purpose of this study is to form the basis for a project on the computer recognition of linear features which are of geological interest, commonly referred to as lineaments. Lineaments are naturally occurring line-like features in the terrain that are inferred to be manifestations of faults or joints. Finding lineaments is of interest not only because of their geological significance, but also because of their usefulness in areas such as environmental geology, mineral exploration, and in the identification of hazards [Short and Lowman, 1973].

III. BASIC ALGORITHMS

Various researchers [e.g., Prewitt, 1970, p. 113] have used linear detectors (or templates); for example, a mask of the form

$$\begin{matrix} -\frac{1}{2} & 1 & \frac{1}{2} \\ -\frac{1}{2} & 1 & \frac{1}{2} \\ -\frac{1}{2} & 1 & \frac{1}{2} \end{matrix},$$

for detecting a vertical line in a 3x3 neighborhood. This means that, if the picture gray levels in the neighborhood of the point e are

$$\begin{matrix} a & b & c \\ d & e & f \\ g & h & i \end{matrix}$$

then we compute $(b+e+h)-\frac{1}{2}(a+d+g+c+f+i)$, and decide that a vertical line is present at e if the value of this expression is sufficiently high.

Rosenfeld [1970, 1971] proposed the use of a nonlinear detector for finding (dark) lines. A nonlinear detector looks for points which satisfy two properties. They must be darker than the neighbors in the direction across the line, and they

must have neighbors in the direction along the line which also possess this property.

To compare these two algorithms let us look more closely at the vertical case. Suppose that the detector is looking for a line at the center of the region labeled B in Figure 1.a. The linear detector requires that the average in B be greater than the average in AUC by some threshold, which we denote by $|B| > |AUC|$. The nonlinear detector divides the regions into zones (three zones are illustrated in Figure 1b), and requires the averages in each of the zones of region B be greater than the averages of the corresponding zones in both A and C by some threshold.

The semilinear detector [VanderBrug, 1975] is a compromise between the above two detectors, and requires the average in B to be greater than the averages in both A and C by some threshold (see Figure 1.c). Such a detector is similar to the nonlinear detector in that it makes separate comparisons to the left and to the right, but does not partition the regions into zones, as is done by the nonlinear detector.

Because the linear detector only requires the region along the line to be darker than the average of the adjacent regions, it will:

1) respond to edges -- at an edge between regions which differ by k, it will output k/2.
2) smear out isolated noise points -- at a point which is k darker than the background, it will output k/3, and similarly at the two neighboring points in the direction along the line.

The semilinear detector does not respond to edges, because it makes separate tests for each of the two adjacent regions. However, it does respond to isolated noise points. The nonlinear detector does not respond to isolated noise points, because it also makes separate tests in the direction along the line. On the other hand, this same feature is a disadvantage of the nonlinear detector when dealing with short gaps in a line.

To examine the relative performance of the three types of line detectors in a controlled environment a set of pictures which contain a vertical line in normally distributed noise ($\mu = 32$, $\sigma = 9$ in a gray scale of 0 to 63) was generated. Pictures with the line intensity equal to one, two, and three standard deviations above the mean of the noise were used in the experiments.

For these experiments the output of each of the detectors is taken to be (1) zero, when the conditions for a line being present are not met; (2) the average over all comparisons made by respective detector, when the conditions for a line being present are met. Thus the detectors do not differ in the magnitude of their response, but only in the conditions under which they will produce a nonzero response.

The original pictures, along with the results of applying all three types of detectors for thresholds of 1, 2, 4, and 8, are shown in Figure 2. The layout of these pictures is illustrated in Figure 2.a. The notation uses L, S, and N for the detectors, with the integer postfix representing the threshold.

None of the detectors performed very well when the line intensity was only one standard deviation above the mean of the noise (see Figure 2.b). The nonlinear detector completely missed the line. The line is visible in the linear and semilinear output for thresholds of 1, 2, and 4; but much of the noise also survives at these low thresholds.

From Figure 2.c one observes that the linear and semilinear detectors for thresholds of 1, 2, 4, and 8 are quite consistent. However, close inspection shown that somewhat more noise points survive in the linear case. The nonlinear detector for thresholds of 1 and 2 cleans up most of the noise, but it also introduces large gaps in the line.

The pictures of Figure 2.d show that the linear and semilinear detectors produce similar results, with the semilinear preserving slightly less noise at all thresholds. The nonlinear detector with threshold 2 found all of the line and responsed to less noise than the semilinear detector with threshold 8.

Much of the noise that remains after one application of a nonlinear detector can be removed by iteration. Figure 3 shows the results of one (Figure 3a) and two (Figure 3b) iterations. The line is getting shorter because the endpoints of a line do not satisfy the criteria of the nonlinear detector.

The experiments confirm that semilinear detectors are slightly superior to linear detectors. This superiority would be more apparent in a set of pictures containing an edge, since the linear detectors would incorrectly respond to the edge. The comparison between semilinear and nonlinear detectors is not as clear cut. Semilinear detectors are not as easily distracted by adjacent noise points, and

more inclined to bridge small gaps in the line. On the other hand, nonlinear detectors do not smear out isolated noise points, and can be used iteratively to clean up noisy output of the detector.

IV. EXPERIMENTS ON SATELLITE IMAGERY

The primary purpose of this paper is to experiment with the semilinear and nonlinear detectors on satellite imagery. It was felt that the slight difference in the performance of the linear and semilinear detectors in the controlled experiments, plus the fact that linear detectors will respond to an edge, was sufficient reason not to experiment with linear detectors on the satellite imagery.

Before discussing the data and the results, we briefly mention how the detectors extend to all orientations. The computation at each point is composed of vertical and horizontal components. There are seven vertical and seven horizontal calculations, as shown in Figure 4. The notation a, b, c refers to the regions A, B, C as used in Figure 1, where we described the algorithms for the vertical case only (i.e., only the single calculation $\begin{matrix} a & b & c \\ a & b & c \\ a & b & c \end{matrix}$. Thus, at each of the 14 calculations, the semilinear detector requires that the average of the b's be greater than the average of the a's by at least the threshold, and the average of the b's be greater than the average of the c's by at least the threshold, in order for the value of that calculation to be nonzero. The final output of the detector is the maximum over the results of the 14 calculations. The orientations for the nonlinear detector are the same as those for the semilinear detector, and each zone consists of one "a", one "b", and one "c".

The images for the experiments came from two sources: Skylab and LANDSAT-1. The Skylab images are from the S190B camera, which is designed to obtain high-resolution color photography. The coverage is of suburban Washington, D. C., and was taken August 1973. Figure 5 is a 255x255 picture of a section of Silver Spring, Maryland. It contains major roads, suburban streets, undeveloped areas, some interesting intersections, and two main commercial districts (in the upper right and the lower left).

Figure 6 is a 255x255 LANDSAT picture from the Tennessee Valley. The coverage is band 6 taken July 1973. The area lies in the transition between the relatively flat line rocks of the Appalachian Plateau and the more steeply folded rocks of the Appalachian Mountains. The linear features in this area are rivers, vegetation alignments, and fractured surface rock which represents faults and joints.

A nonlinear detector that detects 2-point wide lines was implemented. This detector is equivalent to replacing each of the letters in Figure 4 by the average over a 2x2 block of points. When the detector has a nonzero response, that response is stored only in the picture point in the upper left corner of the neighborhood corresponding to the center letter in Figure 4. Placing the nonzero responses in each of the four points would result in extremely thick lines. The detector is applied to every possible 2x2 neighborhood of the picture; that is, it moves across a row (and down a column) one point at a time, not two points at a time.

The result of applying the nonlinear detector with a threshold of 0 to the complement of Figure 5 is shown in Figure 7. It is displayed on a 0 to 63 gray scale. It can be seen that the detector produces mostly low values.

Figure 8a shows a histogram of the lower right quadrant of Figure 7. Approximately 80% of the points have value 0, 16% have values in the range 1 to 5, and less than ½% have values greater than 15. Mapping the points which have value greater than 15 onto 15, multiplying by 4, and complementing Figure 7 produces Figure 9. The amount of distortion introduced by this rescaling process is negligible, since the percentage of points involved is very small.

Figure 9 shows that the nonlinear detector easily found the major streets in Figure 5. Most of these streets are of concrete construction, are four to six lanes wide, and have a small median. The short section which cuts across the exteme lower right is I495, the Capital Beltway. The performance of the detector at intersections is, of course, not very good. This is because the presence of the intersecting street tends to inhibit the output of the detector. The cloverleaf, which is faintly visible in the extreme lower right of the original, was virtually undetected. The triangularly shaped, heavily commercial district in the lower left diminished the output of the detector; however, the outlines of the streets are still quite apparent.

The residential streets in this area are primarily two lane, asphalt roads, with a fair to heavy degree of surrounding vegetation. In spite of this, the detector was able to pick out the basic structure of a number of residential areas, notably the one near the left edge of the picture and the one near the middle, just

above the major street which traverses the picture. It may be that much of the reflectance in the residential areas is due to the rooftops of the houses along the streets.

To accentuate the nonzero responses of the detector a second type of rescaling was done; the constant 31 was added to all of the nonzero values of the picture. This rescaling operation was performed on Figure 7. The complement of the resulting picture is shown in Figure 10. This rescaling drastically distorts the magnitude of the response, but it does not distort the geometry of the response. Figure 10 serves to underscore the fact that the detector was able to determine the basic structure of a number of the residential areas.

The result of applying the nonlinear detector using a threshold of 0 to the LANDSAT picture in Figure 6 is shown in Figure 11. A rescaling operation similar to the first of the two used for the Skylab picture, with a multiplicative factor of 2 instead of 4, produces Figure 12. The basic linear features of Figure 6 do appear in Figure 12. The basic structure of the river which meanders from the top to the bottom of Figure 6 is present. Those sections where it becomes faint correspond to sections in the original where the adjacent areas are as dark as the river. The detector output was low in these areas because, of course, the line was more than two points wide. Also visible in Figure 12 are the linear features which provide the structure of the lineaments in the original picture.

A two point wide semilinear detector was also implemented. It was applied using a threshold of 0 to the lower right quadrant of Figure 5 and the upper right quadrant of Figure 6. The results are shown in Figures 13b and 14b, respectively (the nonlinear detector output for these quadrants appears in Figures 13a and 14a to facilitate comparisons). In both cases the semilinear detector produces significantly wider lines. Also, the fact that the semilinear detector responds to background noise much more readily is apparent from Figure 14. Both the thinner lines and the lack of response to background noise of the nonlinear detector are due to partitioning the regions along the lines into zones. However, this less stringent condition for a nonzero response of the semilinear detector does have its advantages. The residential district in the upper central section of Figure 13 is slightly more visible in the semilinear detector output, (Figure 13b) and hints of the cloverleaf in the lower right are present. The fact that the nonlinear detector shows better response near the borders in Figure 14 should be ignored, because it is solely due to the way it was implemented.

Figure 8a and 8b show histograms of (the unscaled and uncomplemented versions of) Figures 13a and 13b. By comparing these two histograms, one can obtain a quantitative measure of how less stringent the semilinear detector is. The semilinear detector produced about 3/4 the number of 0-values, about three times the number of 1-values, two times the number of 2-values and slightly more of the higher values.

A. DIFFERENT SIZES

To examine the performance of line detectors of different sizes, semilinear detectors of width 1 and 3 were also implemented. The 3-point wide detector records the output only in the middle point of the 3x3 neighborhood which is being examined. Figure 15 shows the results of using the 1, 2, and 3 point wide semilinear detectors, as well as the maximum of these three detectors, applied to the lower right quadrant of Figure 5. Similar pictures for the upper right quadrant of Figure 6 appear in Figure 16. Clearly the 1-point wide detector is too thin, and the 3-point wide detector produces wide responses for the major streets and poor responses for the residential streets. The maximum of the three sizes (Figure 15d) is dominated by the 3-point wide detector (Figure 15c). Figure 15d, the maximum of the three sizes for the LANDSAT picture, has more background noise than any of the individual sizes. In fact, it is virtually a blurred version of the original picture.

Figure 15c illustrates a curious side-effect of using a wide semilinear detector -- the appearance of "shadows" along sections of the major roads. It can be observed that these shadows are most prominent when the line has a diagonal orientation. They arise from the calculations for the orientation which are orthogonal to the line, as illustrated in the following diagram.

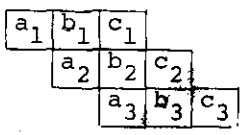

Here the average of the b's exceeds both the average of the a's and the average of the c's, because the line passes right through b_3. Thus the detector places a nonzero value in the center of the 3x3 neighborhood b_3. When the detector is positioned nearer to the line it will have zero (or low) output, because much more of the line will pass through a_3 and c_2. This produces the shadows which

appear in Figure 15c.

Figure 17 is a Skylab picture which has been sampled at every other point. Figure 5 appears in this picture a little below and to the right of center. Applying a 2-point wide detector to Figure 17 is similar to applying a 4-point wide detector to Figure 5. The output of the nonlinear detector applied to Figure 17 is shown in Figure 18. The major streets are all clearly visible, but it is difficult to pick out the structure of any of the residential districts.

I495 cuts across the picture at a 45° degree angle beginning from the upper right, at its intersection with I95. Approximately 3/4 of the way across it almost disappears. However, the road does not actually end at this point; rather, it changes from concrete to asphalt and begins to have not only substantially more foliage on either side, but also foliage in the median. This is an example which illustrates the usefulness of a line follower, because it would tend to want to continue I495 at this point (note that the continuation is faintly visible).

B. DIFFERENT THRESHOLDS

The threshold determines the level of response for which the detector will produce a nonzero output. The experiments with the computer-generated line in noise demonstrated how the choice of threshold can be used to reduce the background noise.

Figure 19 shows the nonlinear detector with thresholds of 1 and 2 applied to the lower left quadrant of Figure 5. Thresholds of 0 (Figure 13a) and 1 do not differ substantially, but a threshold of 2 loses much of the structure of the residential section. Even for threshold 0, there is no noticeable background noise.

The semilinear detector produced a significant amount of background noise in Figure 16b. Figure 20 shows the semilinear detector with thresholds of 4, 8, and 16 applied to this picture. A threshold of 4 leaves most of the background noise; a threshold of 8 removes much of it, without substantially affecting the linear features; while a threshold of 16 destroys most of the linear features.

C. HISTOGRAM FLATTENING

Histogram flattening is a contrast enhancement operation on pictures. For a review of histogram flattening see [Hummel, 1974].

For an n-by-n picture that has m gray levels, we proceed as follows: Let S_0 be the n^2/m points of the original picture f whose gray levels are lowest; say these points have levels $0, 1, \ldots, k_0$, where $k_0 \geq 0$. Then all points of f that have gray levels $0, 1, \ldots, k_0-1$ get gray level 0 in the new picture $\hat{f}$. In addition, just enough points of f that have level k_0 are given level 0 in $\hat{f}$, to make up the desired total of n^2/m. These points can be chosen randomly; or we can rank the points having level k_0 according to the average gray levels of their neighbors, and choose the ones for which this average is lowest. Next, let S_1 be the n^2/m points of f having next lowest gray levels, say, $k_0, k_0+1, \ldots, k_1$, where $k_1 \geq k_0$. We give these points level 1 in $\hat{f}$, resolving ties as just described. The process continues with $S_2, \ldots, S_m$; at the last step, the n^2/m points of f that have the highest gray levels are given level m in $\hat{f}$.

Figure 21 shows the lower right quadrant of Figure 5 (Figure 21a), the results of applying the above operation to this quadrant (Figure 21b), and the output of the nonlinear detector applied to the original picture (Figure 21c) and to the histogram-flattened picture (Figure 21d). Most people can pick out the linear features in the original picture better than in the histogram-flattened picture. But the line detector is able to extract more linear features, at least in the residential areas, from the histogram-flattened picture. A perfunctory examination of a low altitude aerial photograph of this area indicates that most of these additional linear features do reflect the structure of this area. Notice that the main streets are widened to a point where the detector does not find them as well on the histogram-flattened picture.

V. CONCLUSIONS

A number of useful conclusions can be drawn from this study. The semilinear detector is slightly superior to the linear detector, and also has the advantage of not responding to edges. However, the semilinear detector responds to considerably more background noise, and produces slightly thicker lines than the nonlinear detector. The tendency of the nonlinear detector to produce gaps in a line did not manifest itself significantly in either the Skylab or the LANDSAT images.

Both of the detectors were able to pick out the basic structure of the linear features in the terrain of the LANDSAT

images, and (even) in some of the residential sections of the Skylab images. Properly chosen sizes and thresholds are essential to the performance; however, the nonlinear detector usually works quite well with low thresholds. Histogram flattening can be a useful preprocessing operation.

REFERENCES

Bajcsy, R. and M. Tavakoli [1973]; A computer recognition of bridges, islands, rivers, and lakes from satellite pictures, Proc. of Machine Processing of Remotely Sensed Data, Oct. 1973, pp. 2A-54-2A-68.

Bajcsy, R. and M. Tavakoli [1974]; Computer recognition of roads from satellite pictures, Proc. of Second Inter. Joint Conf. on Pattern Recognition, Aug. 1974, pp. 190-194.

Eberlein, R., G. J. VanderBrug, A. Rosenfeld, and L. S. Davis [1974]; Edge and line detection in ERTS imagery: a comparative study, TR-312, Computer Science Center, U. of Maryland, June 1974.

Hummel, R. A. [1974]; Histogram modification techniques, TR-329, Computer Science Center, U. of Maryland, Sept. 1974.

Prewitt, J. M. S. [1970]; Object enhancement and extraction, Picture Processing and Psychopictorics, Academic Press, New York, 1970, pp. 75-149.

Rosenfeld, A., Y. H. Lee, and R. B. Thomas [1970]; Edge and curve detection for texture discrimination, ibid. pp. 381-393.

Rosenfeld, A. and M. Thurston [1971]; Edge and curve detection for visual scene analysis, IEEE Trans. on Computers C-20, 1971, pp. 562-569.

Short, N. M. [1973]; Mineral resources, geological structure and landform surveys, Proc. of Third Earth Resources Symposium, vol. II, Dec. 1973, pp. 147-168.

VanderBrug, G. J. [1975]; Semilinear line detectors, to appear in Computer Graphics and Image Processing.

The support of the National Science Foundation, under Grant GJ-32258X; the help of A. Rosenfeld, A. Blumenthal, and S. Rowe in preparing this report; and the assistance of the Earth Satellite Corp. in obtaining the images is gratefully acknowledged.

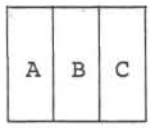

$|B| \succ |A \cup C|$

(1a)

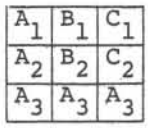

$[|B_2| \succ |A_2| \text{ and } |B_2| \succ |C_2|]$

$[|B_1| \succ |A_1| \text{ and } |B_1| \succ |C_1|]$

$[|B_3| \succ |A_3| \text{ and } |B_3| \succ |C_3|]$

(1b)

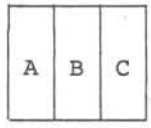

$|B| \succ |A| \text{ and } |B| \succ |C|$

(1c)

Figure 1. Description of the linear (1a), the nonlinear (1b), and the semilinear (1c) detectors for the vertical case.

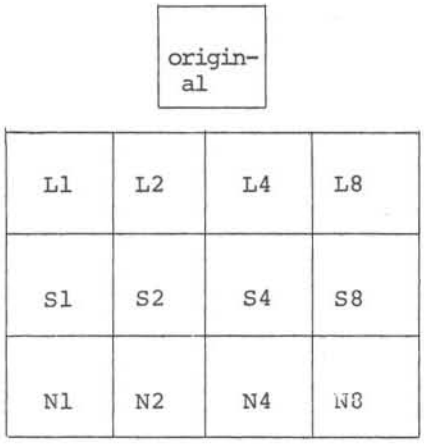

(2a)

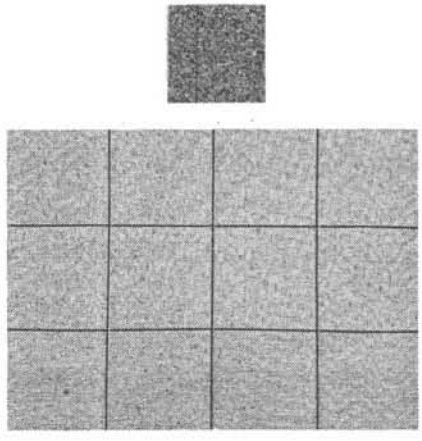

(2b)

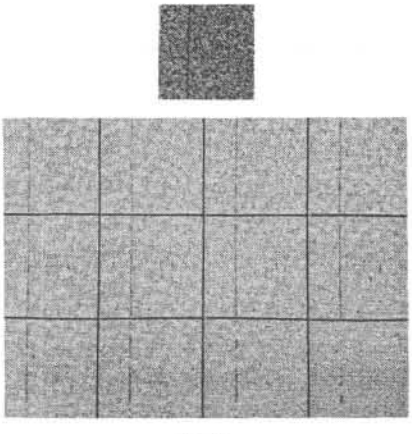

(2c)

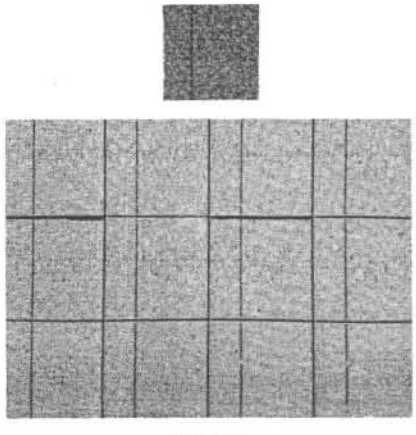

(2d)

Figure 2. Results of the experiments on the computer generated pictures. Figure 2a gives the layout of the other figures. The linear, semi-linear, and nonlinear detectors are denoted by L, S, and N respectively. The suffix indicates the threshold. The originals contain a line having intensity one (2b), two (2c), and three (2d) deviations above the mean of the noise.

(3a) (3b)

Figure 3. Iterating one (3a) and two (3b) times with a nonlinear detector

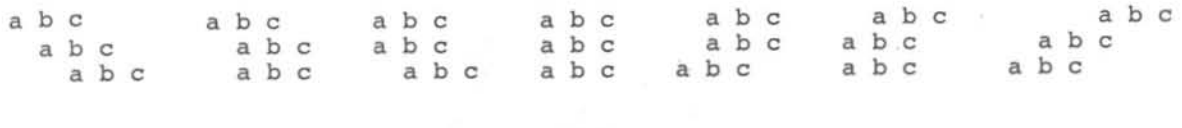

(4a)

(4b)

Figure 4. The seven vertical (4a) and the seven horizontal (4b) calculations that make up a line detection computation at a single point.

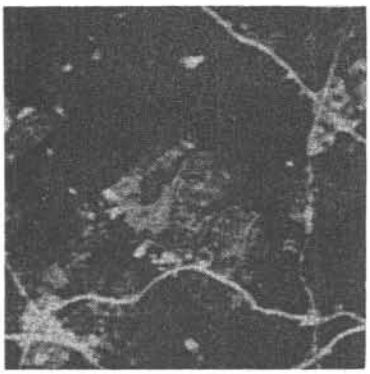

Figure 5. A 255x255 Skylab picture of Silver Spring, Maryland

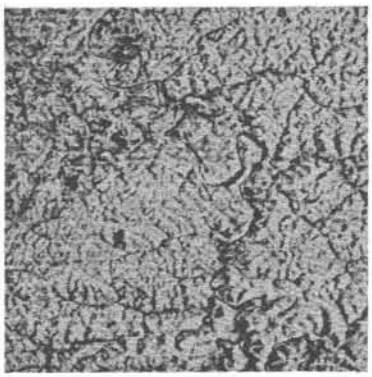

Figure 6. A 255x255 LANDSAT picture from the Tennessee Valley.

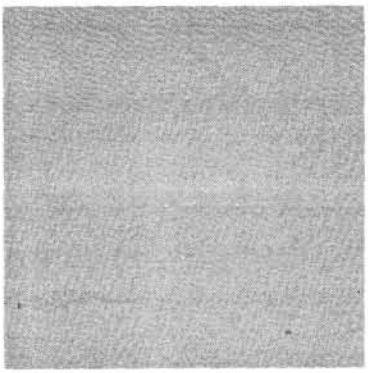

Figure 7. The unscaled output of the nonlinear detector applied to the complement of Figure 5.

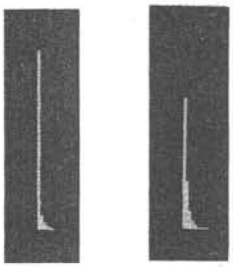

(8a) (8b)

Figure 8. The histogram of the lower right quadrant of Fig. 7, shown in (8a); and the histogram of the semilinear detector output for this same quadrant (of Fig. 5).

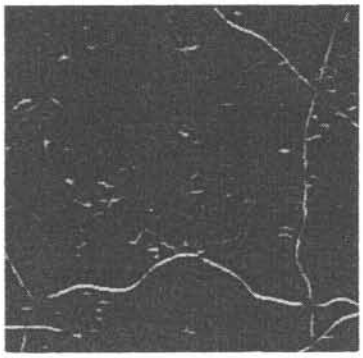

Figure 9. The scaled output of the nonlinear detector applied to Fig. 5.

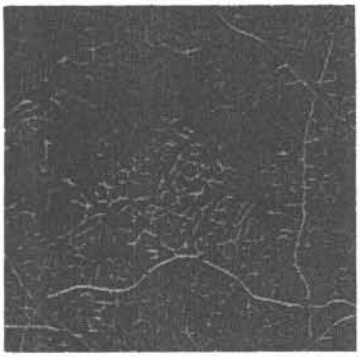

Figure 10. A scaling operation which accentuates the nonzero responses of the detector.

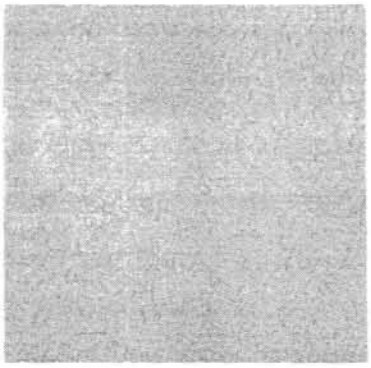

Figure 11. The unscaled output of the nonlinear detector applied to Fig. 6.

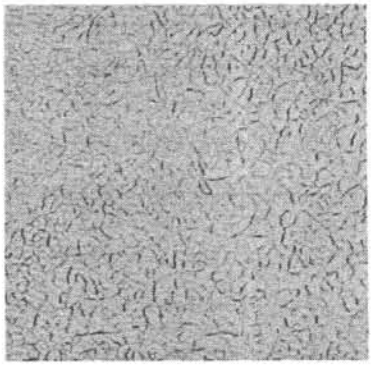

Figure 12. The scaled output of the nonlinear detector applied to Fig. 6.

(13a)

(13b)

Figure 13. The 2-point wide nonlinear (13a) and semilinear (13b) detectors applied to lower right quadrant of Fig.5.

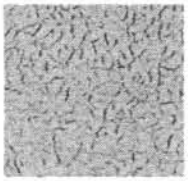

(14a)

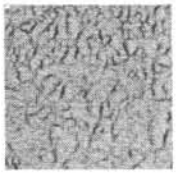

(14b)

Figure 14. Same as Fig. 13 for upper right quadrant of Fig. 6.

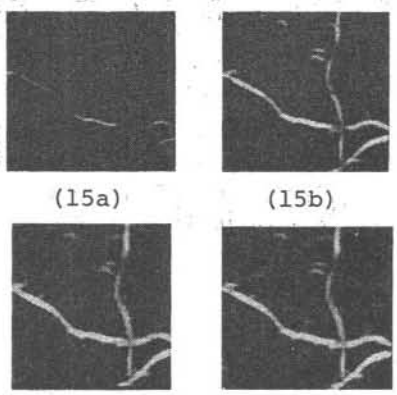

(15a) (15b)

(15c) (15d)

Figure 15. Output of the 1-point (15b), 3-3-point (15c), and the maximum of 1-point, 2-point, and 3-point (15d) semilinear detector applied to lower right quadrant of Fig. 5.

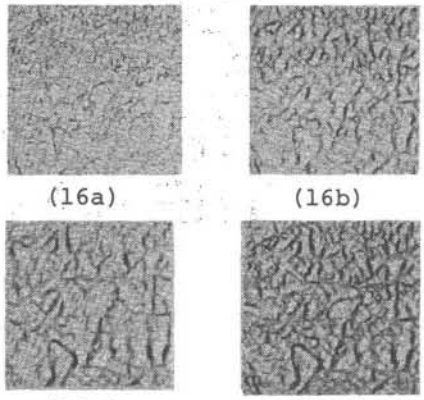

(16a) (16b)

(16c) (16d)

Figure 16. Same as Fig. 15 for the upper right quadrant of Fig. 6.

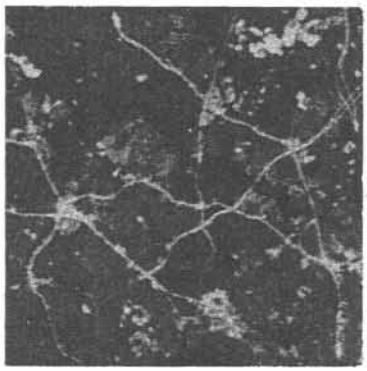

Figure 17. A sampled Skylab picture.

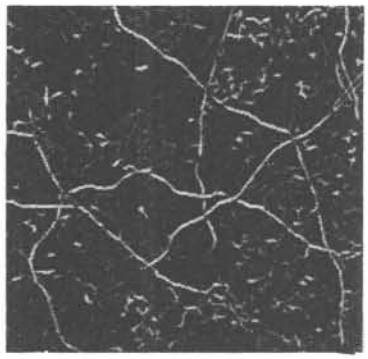

Figure 18. Output of the non-linear detector applied to Fig. 17.

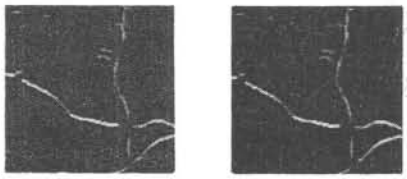

(19a) (19b)

Figure 19. Output of nonlinear detector for thresholds of 1(19a) and 2(19b).

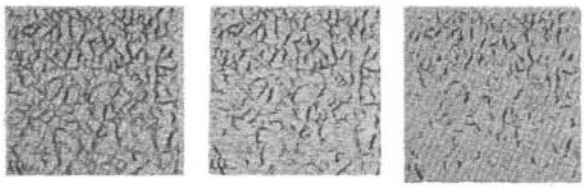

(20a) (20b) (20c)

Figure 20. Output of the semilinear detector for thresholds of 4(20a), 8(20b), and 16(20c).

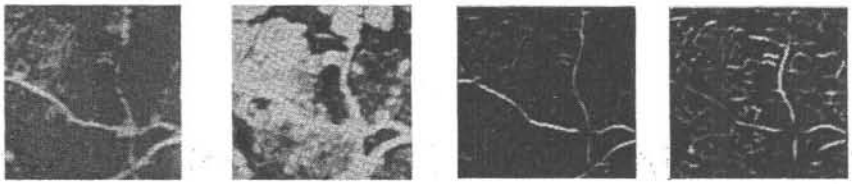

(21a) (21b) (21c) (21d)

Figure 21. An illustration of histogram flattening as a preprocessing operation.

ACREAGE ESTIMATION, FEATURE SELECTION, AND SIGNATURE EXTENSION DEPENDENT UPON THE MAXIMUM LIKELIHOOD DECISION RULE

by J.A. QUIREIN

LACIE VERIFICATION DEPARTMENT
LOCKHEED ELECTRONICS COMPANY
AEROSPACE SYSTEMS DIVISION
16811 EL CAMINO REAL
HOUSTON, TEXAS 77058

M.C. TRICHEL

EARTH OBSERVATIONS DIVISION
SCIENCE AND APPLICATIONS DIRECTORATE
National Aeronautics and Space Administration
LYNDON B. JOHNSON SPACE CENTER
Houston, Texas

Prepared for

SYMPOSIUM ON MACHINE CLASSIFICATION OF REMOTELY SENSED DATA, LABORATORY FOR APPLICATIONS OF REMOTE SENSING, PURDUE UNIVERSITY, WEST LAFAYETTE, INDIANA
JUNE 3, 1975